Prob. 8.4 Evaporation rate under <u>varying</u> wall temperature for a pulsed reactor: If 0.1 MJ of plasma energy is dumped on 1 m^2 of a 1000 K vanadium reactor wall in 0.1 ms, estimate the peak temperature, number of atoms evaporated by the thermal spike per m^2, and the wall thickness loss.

<u>Ans.</u> The surface temperature rise for an energy dump onto a surface over a brief interval of time is given by

$\Delta T = 2W/S(\pi C_p K \rho_m \tau)^{1/2}$ (K), (cf. lecture note)

where W = energy dump = 0.1 MJ = 1×10^5 J
S = wall surface area for dump = 1 m^2
C_p = specific heat for vanadium @ 1000K = 640 $\frac{J}{kg\,K}$
K = thermal conductivity " @ 1000K = 38.6 W/(m-K) (Table 8.10) (Table 8.10)
ρ_m = density = 5870 kg/m^3 (Table 8.10)
τ = time interval of dump = 0.1 ms = 1×10^{-4} s

$\therefore \Delta T = 937°K$, then the peak temperature is $1000 + \Delta T = \underline{\underline{1937°K}}$

The number of wall atoms evaporated is given by (cf. lecture note)

$\Delta n/S \simeq 0.1\,\tau\,\phi_n(T_{max})$ (atoms/m^2),

where ϕ_n = evaporation flux at the peak temperature
$= 2.6\times10^{24}\,\alpha p/(AT)^{1/2}$ (atoms/m^2·s) (Eq. 8.24)

with α = sticking coefficient $\simeq 1$, p = vapor pressure = 1×10^{1} Pa,
A = atomic weight = 50.942 g/mole, T = 1937 K (Fig. 8.25).

then $\phi_n(T_{max}) = 8.277\times10^{20}$ atoms/(m^2·s)

$\therefore \Delta n/S = 0.1\,(1\times10^{-4}\,s)(8.277\times10^{20}\ \text{atoms}/(m^2\cdot s)) = \underline{\underline{8.28\times10^{15}\ \text{atoms}/m^2}}$

The wall thickness loss due to the evaporation of these atoms is

$\Delta x = \dfrac{\Delta n/S}{n_w} = \dfrac{\#\text{ of atoms evaporated per unit area}}{\#\text{ of wall atoms per unit volume}}$,

where $n_w = 6.93\times10^{28}$ atoms/m^3 for vanadium (cf. Table 8.10)

$\therefore \Delta x = \dfrac{8.28\times10^{15}\ \text{atoms}/m^2}{6.93\times10^{28}\ \text{atoms}/m^3} = \underline{\underline{1.19\times10^{-13}\ m}}$

[Note for a <u>constant</u> wall temperature @ 1600°K for vanadium wall (cf. Example 8.4)
$dx/dt = 1.7\times10^{-11}$ m/s = 0.54 mm/a, too high wall erosion!]

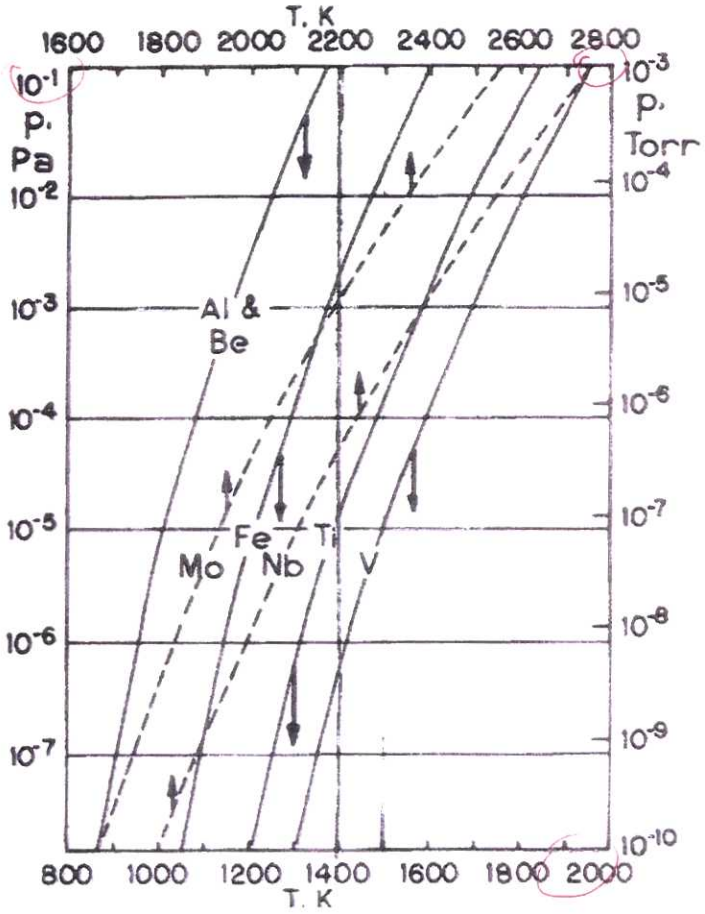

Fig. 8.25 Equilibrium vapor pressure for various wall materials versus temperature. For dashed curves read the top temperature scale (Based on data of Honig and Kramer 1969)

Table 8.10 Thermal properties of various materials. Data are from Behrisch (1972), Table 1

		V	Nb	Mo	C	SS 304
Z, atomic number		23	41	42	6	18 % Cr
A, atomic mass (gm/mole)		50.94	92.9	95.94	12	8 % Ni
ρ_m, mass density (kg/m^3)		5,870	8,570	9,010	2,250	7,900
n_w, atomic density (10^{28} atoms/m^3)		6.93	5.56	5.65	11.3	8.6
T_m, melting temperature (K)		2,192	2,688	2,883	(vap.) 3,925	1,400
ΔH, heat of sublimation (eV/atom)	300 K	5.33	7.5	6.83	8.2–10.4	
	500 K	5.27	7.43	6.78		
	1,000 K	5.16	7.28	6.63		
	1,500 K	4.96	7.14	6.48		
	2,000 K	4.75	6.97	6.3		
k, thermal conductivity (W/m K)	500 K	33.1	56.7	130	80–100	19
	1,000 K	38.6	64.4	112	49–64	
	1,500 K	44.7	72.1	97	40–50	
	2,000 K	50.9	79.1	88	30–40	
c_P, specific heat (J/kg K)	500 K	500	280	254	1,200	500
	1,000 K	640	300	290	1,670	
	1,500 K	700	330	330	1,800	
	2,000 K	850	370	380	2,000	

C. Plasma Materials Interactions (cont'd)

iii) Near-surface wall modifications

- Phase changes – can occur in surface films (e.g., as oxides, carbides, and hydrides) and also occur internally (e.g., strain-induced austenitic-martensitic transformation in stainless steels). Flaking and hydrogen cracking may result from the changes of thermal conductivity and the steel's mechanical properties, respectively.

- Alloy composition changes – nuclear transmutations (in both gaseous and solid transmutants), preferential sputtering (with high sputtering yield elements preferentially removed from the surface of an alloy), and diffusion+surface segregation (impurities like carbon diffuse to the surface where they are desorbed or sputtered away; in stainless steel, chromium segregates to the surface as an oxide.)

- microstructural changes – in addition to neutron-induced radiation damage, ion impact produces vacancies, interstitials, and dislocation loops in the first 10 nm of the surface; these defects lead to internal stress, swelling, creep, recrystallization and grain growth, and tritium trapping in the near-surface.

- macrostructural changes – include nonuniform erosion and redeposition (cf. building up flakes), cracking, topological changes (cf. blistering, exfoliation (intergranular corrosion), sputtering (yielding a honeycomb-like surface)), and tungsten fuzz (creating a fuzzy surface under high heat flux) ← may have lower sputtering rate

- Property changes – may affect physical properties (electrical and thermal conductivity, emissivity, density, optical reflectivity, radioactivity, work function, and magnetic permeability) and mechanical properties (ductility, creep rate, crack growth rate)

D. PFC (Plasma Facing Components)

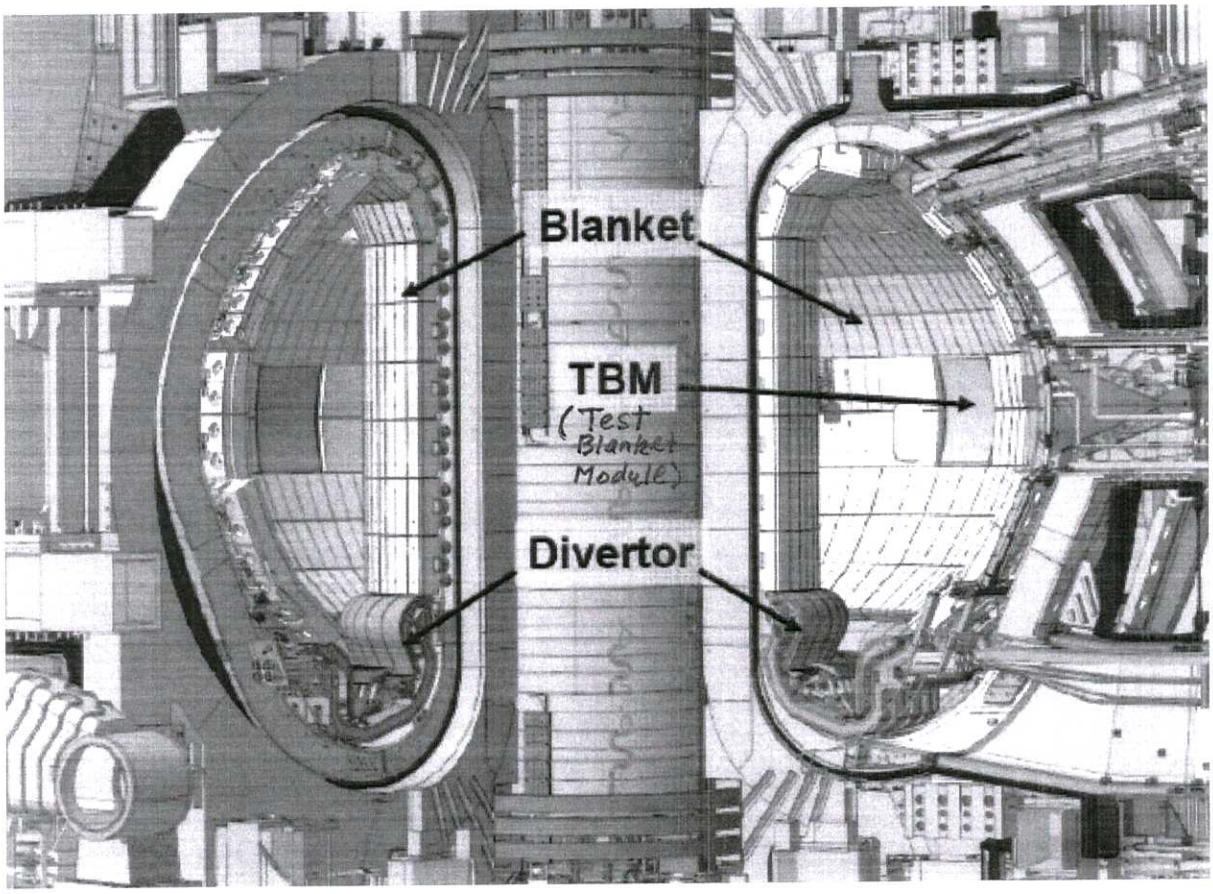

Fig. 1. ITER Plasma facing components
[Ref. M. Merola, et al., ITER plasma-faring components, Fusion Engrg & Design 85 (2010) 2312-2322.]

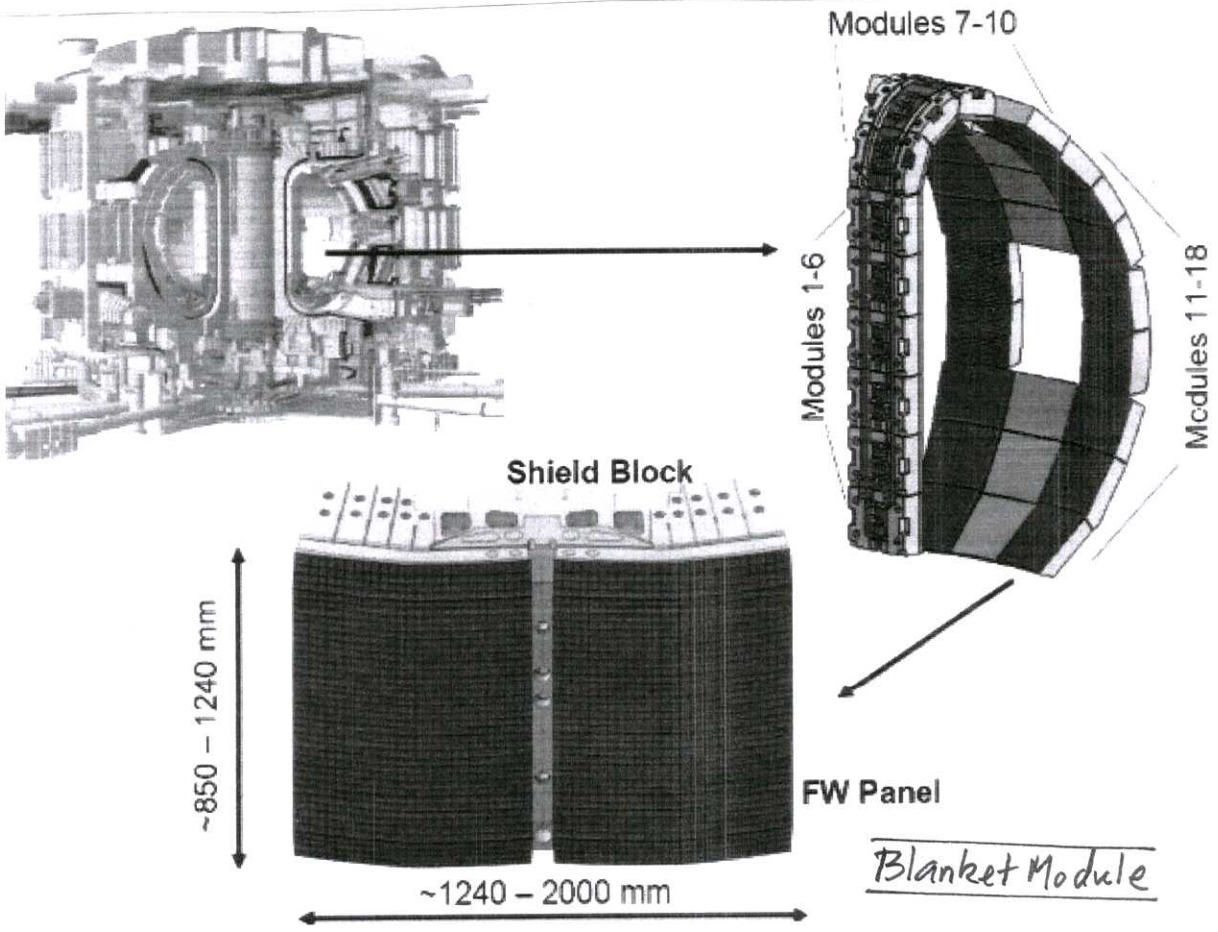

Blanket design

Table 1
Summary of main blanket design parameters.

Parameter	Value
Number of BMs	440
Typical module dimension	1.4 m × 1.0 m × 0.45 m
Max allowable mass of one module	4.5 t
Total mass on BMs	1530 t
Coolant type	Water
Inlet temperature (°C)	100
Inlet pressure at chimney bulk head (MPa)	3.0
Minimum FW panel flow velocity (m/s)	1.5
Minimum SB flow velocity (m/s)	0.8
Materials	
Heat sink of FW panels	CuCrZr-IG alloy
Armour	Beryllium (S-65C or equivalent)
Pipes and hydraulic connections	316L
Shield block	316L(N)-IG
Design heat flux on FW panels	1–2 and 5 MW/m^2 depending on location
Max neutron damage in Be/heat sink/steel pipe/SB	1.6/5.3/3.4/2.3 dpa

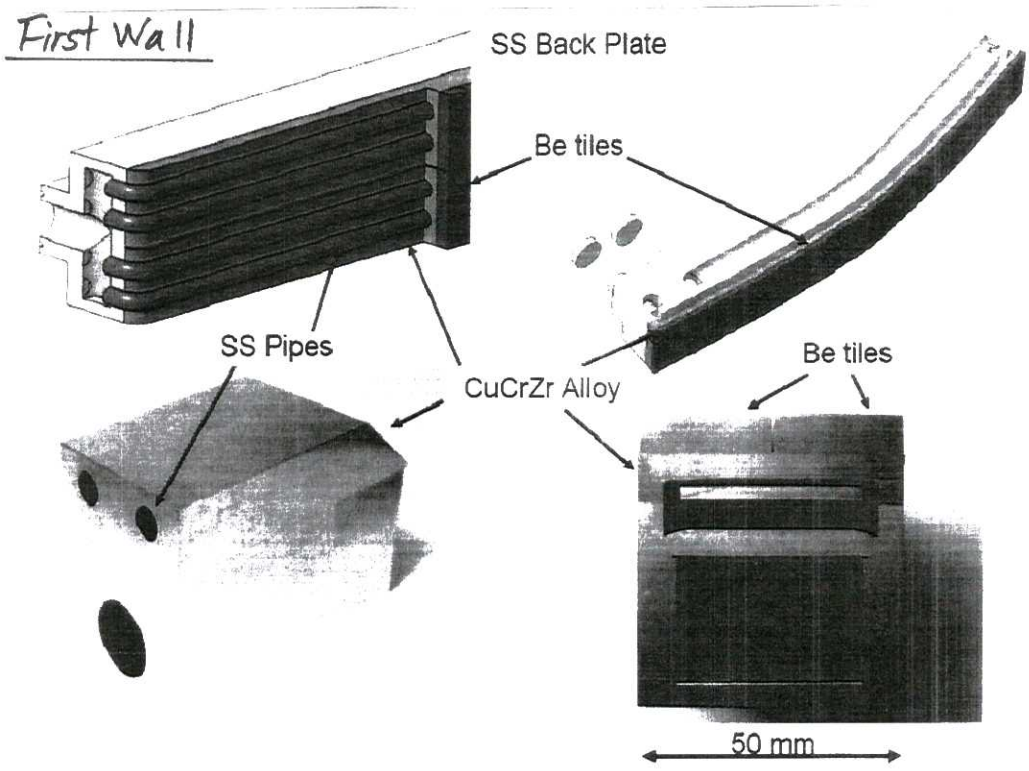

Fig. 3. Illustration of the basic FW panel structure and fingers. Left: normal heat flux fingers (concept with steel cooling pipes). Right: enhanced heat flux fingers (concept with rectangular channels).

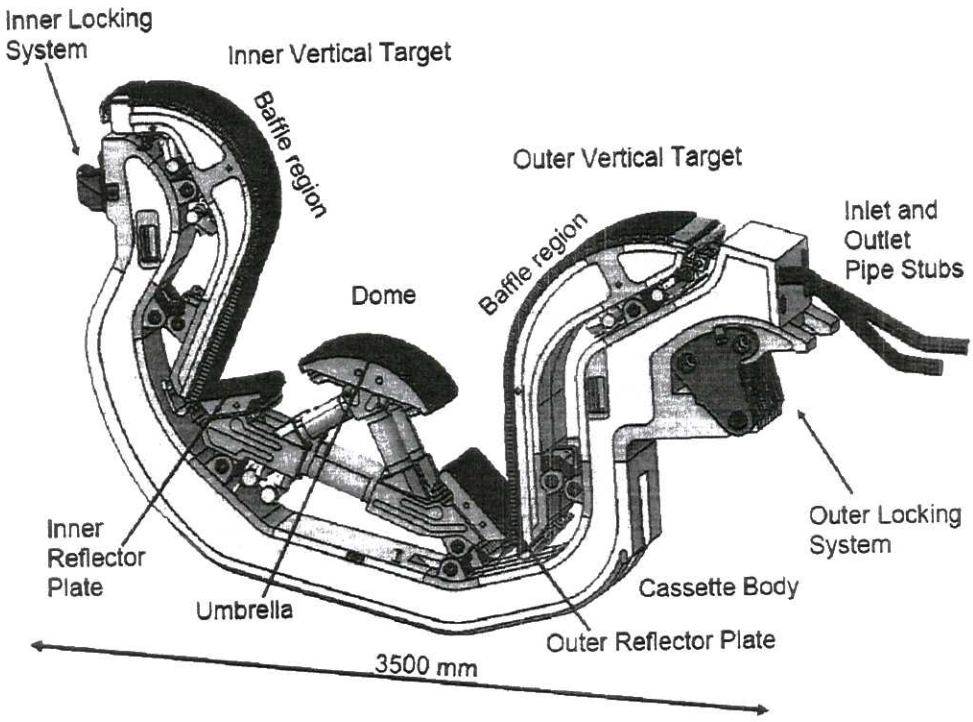

Fig. 6. Divertor cassette assembly.

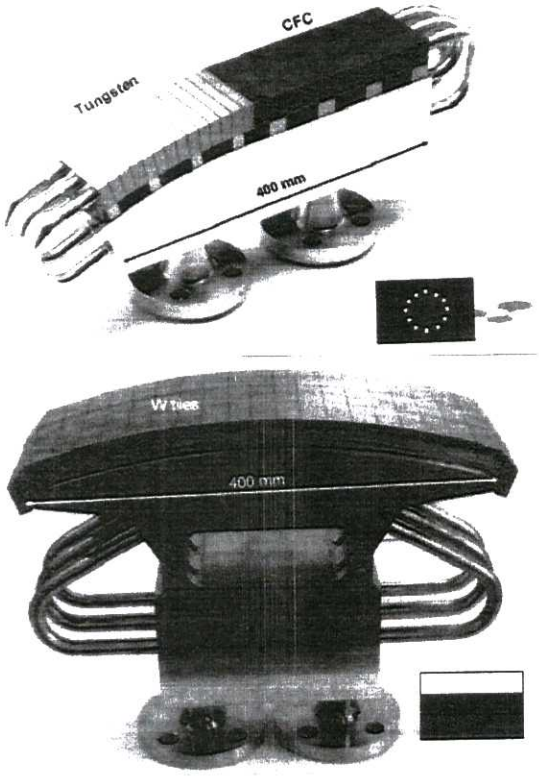

Fig. 8. Vertical target (top) and dome (bottom) medium-scale prototypes.

Table 2
Summary of main divertor design parameters.

Parameter	Value
Size	
Toroidal extent of a cassette	6.67°
Number of cassettes	54
Coolant type	Water
Inlet temperature (°C)	100
Inlet pressure at pipe stubs (MPa)	4.2
Max permissible pressure drop (MPa)	1.6
Max permissible total flow rate (kg/s)	1000
Materials	
Cassette body and supporting structures of PFCs	SS 316L(N)-IG and XM-19
Heat sink of PFUs	CuCrZr-IG alloy
Armour	CFC, pure sintered and deformed W
Pipes	316L
Pins of multilink attachments	C63200 Ni-Al bronze
Inner and outer locking system: nose and knuckle	C63200 Ni-Al bronze
Hard cover plates of divertor rails	Steel 660
Shear pins of hard cover plates	C63200 Ni-Al bronze
Design load for target in strike point region	~10 MW/m^2
Design load of target in baffle region	~5 MW/m^2
Min critical heat flux margin	1.4
Thickness of carbon fibre composite (CFC) at end of life	>4 mm
Plasma-facing surface area	~190 m^2

Test Blanket Module (TBM)

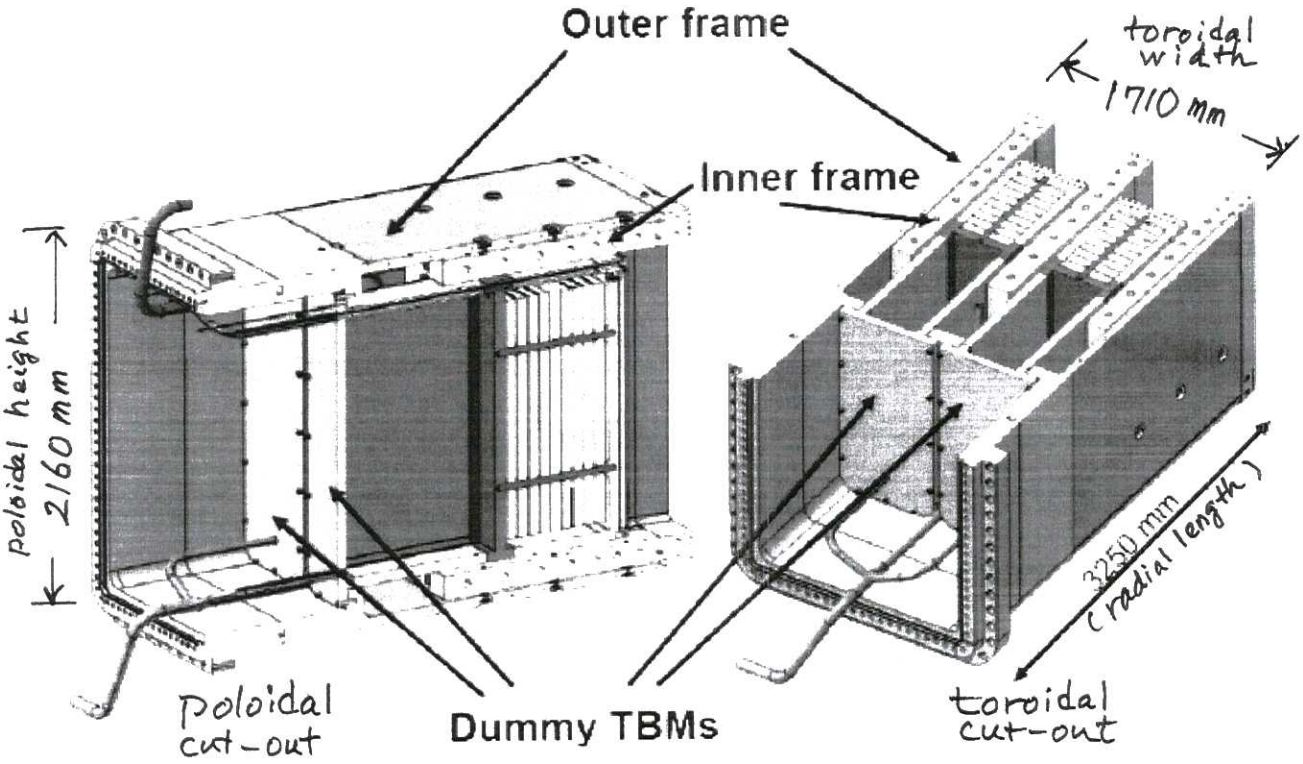

The TBM frame is a water-cooled 316L(N)-IG steel port structure, which is based on the same materials and manufacturing process as those used for the blanket shield block (SB).

Note: Attached references on plasma-facing components, i.e., M. Merola, et al., ITER plasma-facing components, Fusion Engineering & Design 85 (2010) 2312-2322; D. Stork, et al., Developing .... plasma facing materials; Journal of Nuclear Materials 455 (2014) 277-291; and V. Philipps, Tungsten as material for plasma-facing components in fusion devices, Journal of Nuclear Materials 415 (2011) 52-59.

§ 8.10 Irradiation Facilities

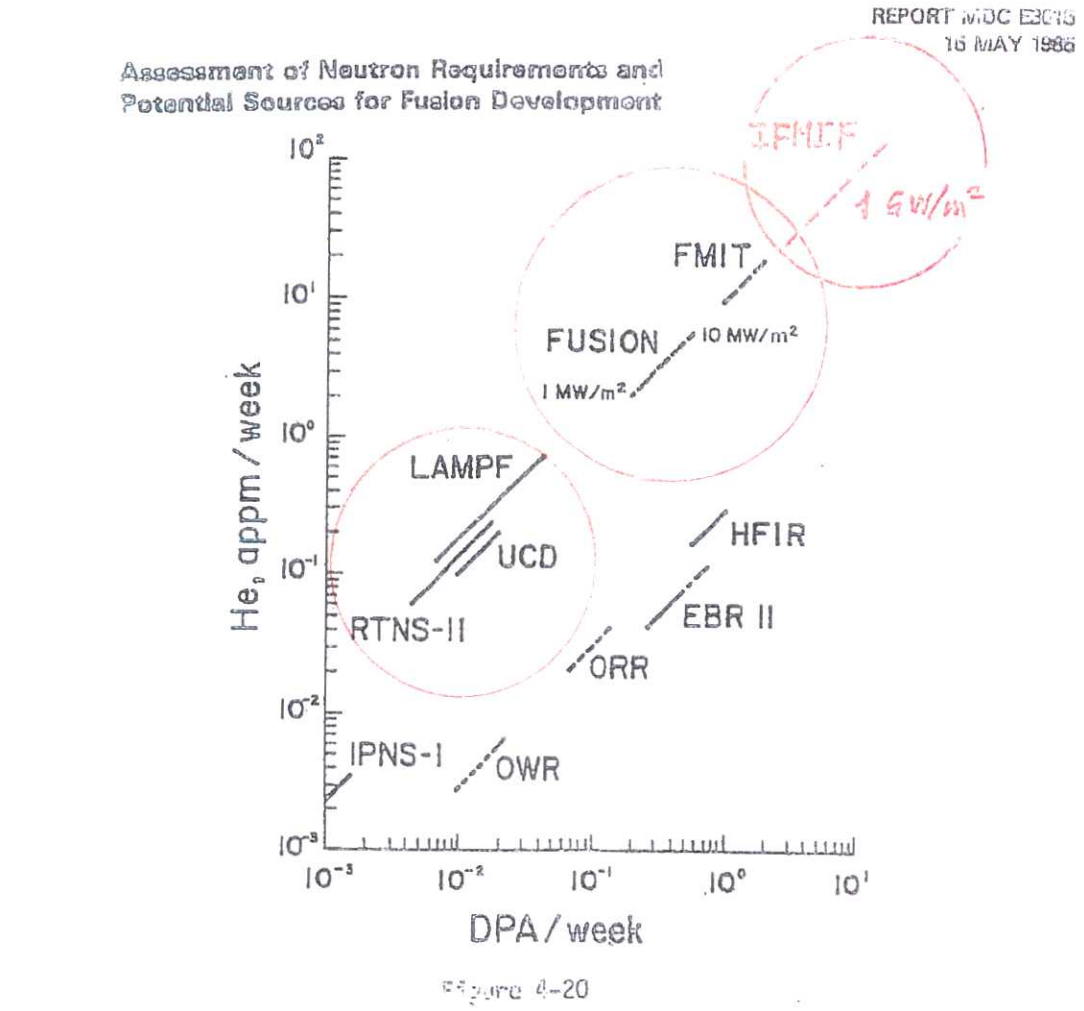

Figure 4-20

Production of He per dpa in Various Neutron Source Devices

Estimate for Neutron Irradiation of 10-50 dpa

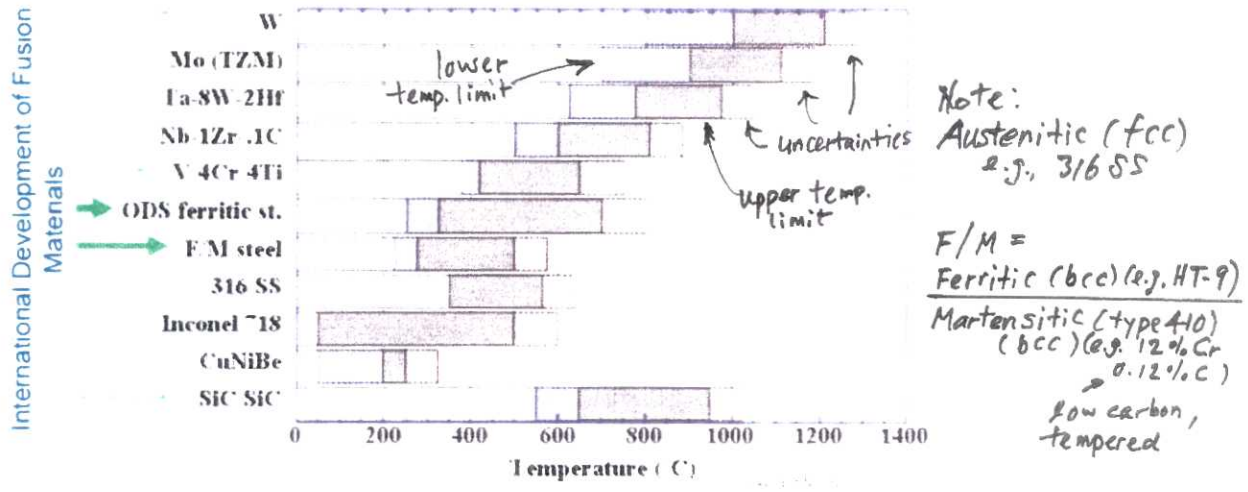

Fig. 8.47 Operating temperatures of some structural materials. Arrows indicate favored materials (Zinkle and Ghoniem 2000)

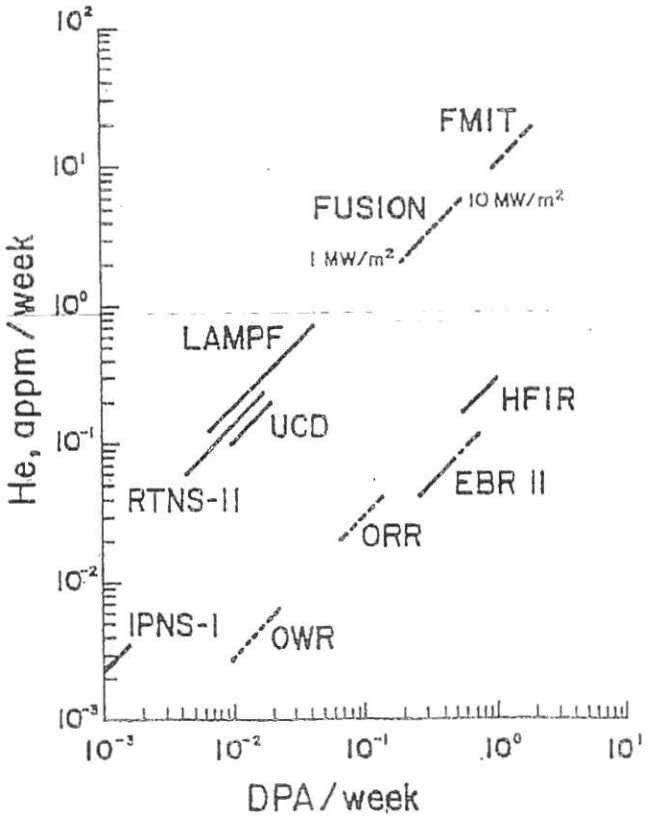

Figure 4-20

Production of He per dpa in Various Neutron Source Devices

ACCELERATOR FLUX (10^{12} n/cm^2 · sec)	EXPERIMENTAL VOLUME (LITERS)				
	< 1	1 - 10	10 - 25	25 - 50	> 50
> 1000	FMIT				
500-1000					LAMPF (U target)
100-500	FMIT				
50-100	UCD				LAMPF (Cu target)
10-50	RTNS-II				
5-10					
< 5	IPNS-I (REF)				

Experiment volume(liters)

Fast Flux (n/cm^2 · sec)	<1	1-10	10-25	25-50	50-75	75-100	100-200	200-350	>350
$>10^{15}$		FFTF EBR-II		FFTF					
$5x10^{14}-10^{15}$	HFIR	HIFR							
$10^{14}-5x10^{14}$	NSBR HFIR HFBR MITR ATR	ETR,ATR GETR ORR,HFIR MITR,HFR	ETR	ETR					ETR
$5x10^{13}-10^{14}$									
$10^{13}-5x10^{13}$	MURR	OWR	PBR					ORR	
$5x10^{12}-10^{13}$		BSR							
$<5x10^{12}$		ATR	ATR					ATR	

LIST OF ACRONYMS

ACRONYM	DEFINITION
ADIP	Alloy Development for Irradiation Performance
ANL	Argonne National Laboratory
ATR	Advance Test Reactor
BANG	Brookhaven Accelerator-Based Neutron Generator
BCSS	Blanket Comparison and Selection Study
BNL	Brookhaven National Laboratory
CCT	Center Cracked Tension
CLIRA	Closed Loop in Reactor Assembly
CRFPR	Compact Reversed-Field Pinch Reactor
CRNL	Chalk River National Laboratory
CW	Continuous Wave
DAFS	Damage Analysis and Fundamental Studies
DBTT	Ductile Brittle Transition Temperature
d.c.	Direct Current
DEMO	Fusion Demonstration Reactor
DOE	Department of Energy
dpa	Displacement per atom
DT	Deuterium-tritium
EBR-II	Experimental Breeder Reactor-II
ECRH	Electron Cyclotron Resonance Heating
EOL	End of Life
e.p.	Electro-Potential
EPRI	Electric Power Research Institute
ETEC	Energy Technology Engineering Center
ETF	Engineering Test Facility
ETR	Engineering Test Reactor
FED	Fusion Engineering Device
FERF	Fusion Engineering Research Facility
FFTF	Fast Flux Test Facility
FMIT	Fusion Materials Irradiation Test Facility
FWB	First Wall/Blanket
GA	GA Technologies, Inc.
GETR	General Electric Test Reactor
HEDL	Hanford Engineering Development Laboratory
HFBR	High Flux Beam Research Reactor
HFIR	High Flux Isotope Reactor
HFR	High Flux Reactor
ING	Intense Neutron Generator
INGRID	Intense Neutron Generator for Radiation-Induced Damage
INS	Intense Neutron Source
INTOR	International Torus
IPNS	Intense Pulsed Neutron Source
ITR	Ignition Test Reactor
JAERI	Japanese Atomic Energy Research Institute
JET	Joint European Torus
JMTR	Japan Materials Testing Reactor
KARIN	Karlsruhe Ring-Ion-Source Neutron Generator
LAMPF	Los Alamos Meson Physics Facility
LANL	Los Alamos National Laboratory
LASREF	Los Alamos Spallation Radiation Effects Facility
LLNL	Lawrence Livermore National Laboratory
LOCA	Loss of Coolant Accident
MARS	Mirror Advanced Reactor Study
MCF	Magnetic Confinement Fusion
MDAC	McDonnell Douglas Astronautics Company
MFR	Magnetic Fusion Reactor
MFTF α+T	Mirror Fusion Test Facility Upgrade
MFTF-B	Mirror Fusion Test Facility (Tandem Configuration)
MHD	Magnetohydrodynamic
MIT	Massachusetts Institute of Technology
MITR	Massachusetts Institute of Technology Reactor
MOTA	Materials Open Test Assembly
MTR	Materials Test Reactor
MURR	University of Missouri Reactor
NBINS	Neutralized-Beam Intense Neutron Source
NRL	Naval Research Laboratory
NSBR	National Bureau of Standards Reactor
OHTE	Ohmically Heated Toroidal Experiment
ORELA	Oak Ridge Electron Linear Accelerator
ORIC	Oak Ridge Isochronous Cyclotron
ORNL	Oak Ridge National Laboratory
ORR	Oak Ridge Research Center
OWR	Omega West Reactor
PCA	Prime Candidate Alloy
PW	Pulsed White
R&D	Research and Development
RCS	Rapid Cycling Synchrotron
REF	Radiation Effects Facility
RFP	Reverse-Field Pinch
RFTP	Field-Reversed Theta Pinch
RTNS	Rotating Target Neutron Source
SCTO-F	Single Coil Technology Demonstration Facility
SNS	Spallation Neutron Source
TDF	Technology Development Facility
TEM	Transmission Electron Microscopy
TETR	Tokamak Engineering Test Reactor
TFTR	Tokamak Fusion Test Reactor
TMR	Tandem Mirror Reactor
TMX	Tandem Mirror Experiment
TNS	The Next Step
TSTA	Tritium Systems Test Assembly
T_m	Absolute Temperature of melt (K or R)
UCD	University of California-Davis
UCLA	University of California-Los Angeles
UNM	University of New Mexico
UTS	Ultimate Tensile Strength
UW	University of Wisconsin
UWMAK-I	University of Wisconsin Tokamak Conceptual Design
VTA	Vertical Test Assemblies
WNR	Weapons Neutron Research Facility
YS	Yield Strength

International Fusion Mat'ls Irradiation Facility :

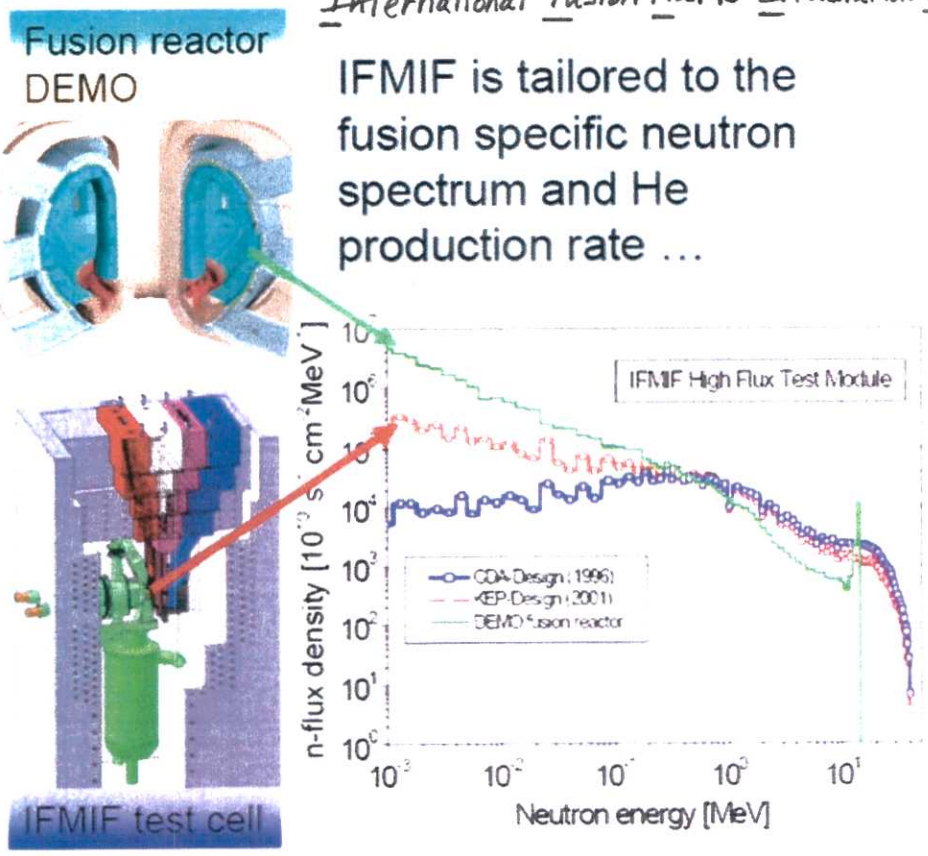

Fig. 8.42 Comparison of predicted IFMIF and DEMO neutron energy spectra (Rieth 2008, From work by A. Möslang, KIT)

The capabilities of IFMIF will be:

- High flux region (V = 0.5 L) $\geq$ 20 dpa/a
- Medium-flux region (V = 6 L) $\geq$1 dpa/fpy [fpy = full power year]
- Temperature control
- Miniaturized specimens
- Post-irradiation examination (PIE)
- Availability $\geq$70 %.

First phase: 3 years, half-intensity

- Screening candidate structural materials
- Calibrating data from fission reactors and ion beams.

} 30-yr facility

Second phase: 20 years, full power test facility

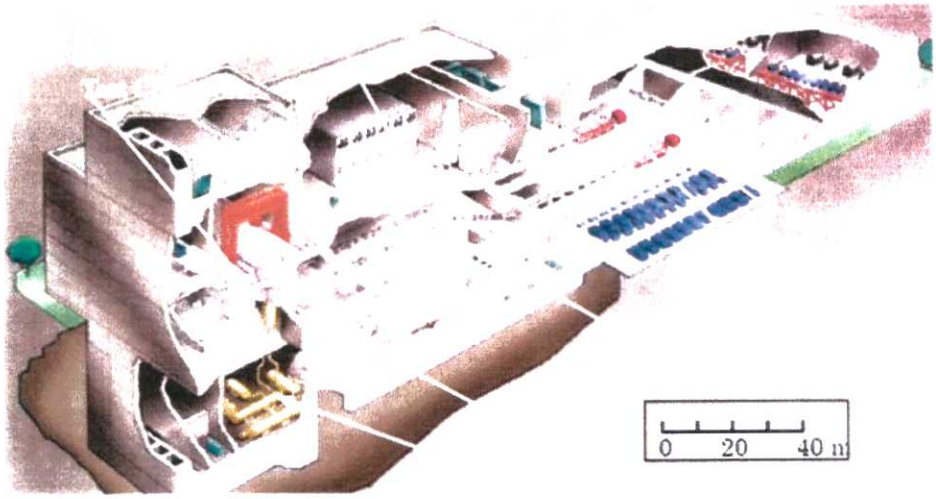

Fig. 8.43 The International Fusion Materials Irradiation Facility (IFMIF 2004)

The main IFMIF parameters :

2 D^+ beams each	40 MeV, 125 mA
Beam deposition area on target	0.2 m × 0.05 m
Jet velocity	15 m/s
Average target heat flux	1 GW/m^2
Li flow rate	130 l/s
Pressure at Li surface	10^{-3} Pa
Hydrogen isotopes content in Li	<10 wppm
Impurity content (each C, N, O)	<10 wppm
Structure	SS-316
Back wall replacement period	11 months
Other components lifetime	30 years
Availability	>95 %

Another future facility –
The European Spallation Source (ESS) in Lund, Sweden :
produce intense neutron source by impact of a 5 MW, 2.5 GeV proton beam onto a tungsten target or Pb-Bi eutectic. [Note: the neutron source spectrum will not match that of a fusion reactor.]

Wall Conditioning :

- Adsorbed atoms have binding energies – ~0.3eV – ~3eV.
- Impurities (e.g., CO and H_2O) are typical adsorbents, besides hydrogen adsorbed on the surfaces.

Impurities can be desorbed by incident ions, neutrals, electrons, and photons. Desorption cross-section ~ 10^{-18} m^2.

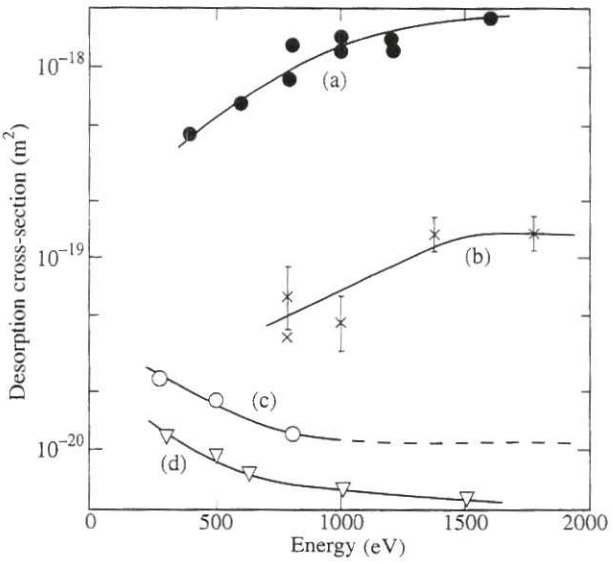

Ref. Wesson, Tokamaks

Fig. 9.6.1 Energy dependence of experimental desorption cross sections: (a) $^4He^+$ incident, carbon monoxide on nickel; (b) $^3He^+$ incident, hydrogen on tungsten; (c) $^4He^+$ incident, hydrogen on molybdenum; (d) H^+ incident, deuterium on nickel (Taglauer, E., in *Nuclear Fusion Special Issue*, ed. Langley, R.A., I.A.E.A., Vienna (1984).)

- Discharge cleaning ← (10–20 MHz) @ 10^{-1} Pa
  glow discharges, pulsed discharges and discharges excited by radiation at electron cyclotron frequency aim to optimize the removal of wall impurities by energetic ions, neutrals, electrons, or photons. [cf. Alcator]

- Thin metallic films (< 10–100 μm)
  Evaporation of wires (e.g., Ti, Cr, Be) at high vapor pressures at typically 1500–2000 °K produces thin metallic films for improving the vacuum (cf. gettering)

- Non-metallic films (~ 1 μm)
  Low Z non-metallic films (e.g., C and B) to coat the walls of tokamaks in order to minimize the release of high Z impurities. (cf. carbonization and boronization)
  Optimum wall temperature is about 300 °C to form a hard, adherent film, typically containing 40% hydrogen.